ANTIOXIDANTS & REDOX SIGNALING
Volume 9, Number 7, 2007

DOI: 10.1089/ars.2007.1526

Original Research Communication

Selective Oxidative Stress in Cell Nuclei by Nuclear-Targeted D-Amino Acid Oxidase

PATRICK J. HALVEY,[1,3] JASON M. HANSEN,[1] JENNIFER M. JOHNSON,[2] YOUNG-MI GO,[2] AFSHIN SAMALI,[3] and DEAN P. JONES[2]

ABSTRACT

The effects of nuclear-localized oxidative stress on both nuclear antioxidant systems, and the processes that they regulate, are not clearly understood. Here, we targeted a hydrogen peroxide (H_2O_2)-producing enzyme, D-amino acid oxidase (DAAO), to the nucleus (NLS-DAAO) and used this to generate H_2O_2 in the nuclei of cells. On addition of *N*-acetyl-D-alanine (NADA), a substrate of DAAO, to NLS-DAAO–transfected HeLa cells, a twofold increase in ROS production relative to untreated, transfected control was observed. Staining of cellular thiols confirmed that NLS-DAAO–induced ROS selectively modified the nuclear thiol pool, whereas the cytoplasmic pool remained unchanged. Furthermore, NLS-DAAO/NADA–induced ROS caused significant oxidation of the nuclear GSH pool, as measured by nuclear protein *S*-glutathionylation (Pr-SSG), but under the same conditions, nuclear Trx1 redox state was not altered significantly. NF-κB reporter activity was diminished by NLS-DAAO/NADA–stimulated nuclear oxidation. We conclude that nuclear GSH is more susceptible to localized oxidation than is nuclear Trx1. Furthermore, the attenuation of NF-κB reporter activity in the absence of nuclear Trx1 oxidation suggests that critical nuclear redox proteins are subject to control by *S*-glutathionylation during oxidative stress in the nucleus. *Antioxid. Redox Signal.* 9, 807–816.

INTRODUCTION

ACCUMULATING EVIDENCE suggests that differential responses in nuclear and cytoplasmic compartments form a basis for selectivity in redox signaling mechanisms (20–22). Generation of reactive oxygen species (ROS) is associated with the binding of certain growth factors and cytokines, such as epidermal growth factor (EGF) and tumor necrosis factor α (TNF-α) to their cell-surface receptors (16, 55). These physiologically derived ROS induce differential, compartmented redox effects (20, 22). In the cytoplasm, several kinase/phosphatase signaling pathways are susceptible to alterations in redox environment [*e.g.*, ASK-1 and protein tyrosine phosphatase (PTP)] (10, 51). Oxidative modification of catalytic cysteines in PTPs by hydrogen peroxide (H_2O_2) results in the transient inhibition of phosphatase activity. In the nucleus, redox-dependent signaling mechanisms play an integral role in regulation of gene expression. Several transcription factors, including NF-κB, p53, and AP-1, possess reversibly oxidizable cysteines in their DNA-binding domains that are subject to modulation via interaction with a redox sensor protein, redox factor 1 (Ref1) (23, 25, 45). Oxidation of these cysteine residues results in a decrease in DNA-binding activity (38). Other redox modifications to cysteines in transcription factor DNA-binding sites include *S*-glutathionylation, *S*-nitrosylation, and sulphenic/sulphonic acid formation (46, 50). Suppression of redox-active transcription factors can be achieved through toxicologic agents, as shown by repression of DNA binding of NF-κB by diamide and *N*-ethyl maleimide (57).

Two major thiol systems function in redox regulation, one dependent on thioredoxin 1 (Trx1) and the other dependent on glutathione (GSH). Trx1 acts as a protein thiol reductant

[1]Division of Pulmonary, Allergy, Cystic Fibrosis and Sleep, Department of Pediatrics; and [2]Division of Pulmonary, Allergy and Critical Care Medicine, Department of Medicine, Emory University School of Medicine, Atlanta, Georgia.
[3]Department of Biochemistry and National Centre for Biomedical Engineering Science, National University of Ireland, Galway, Ireland.

and is an important regulator of redox-sensitive transcription in the nucleus (48). Although it does not contain any nuclear localization sequences, Trx1 translocates into the nucleus in response to hydrogen peroxide, tumor necrosis factor, and ionizing radiation (24, 35, 61). Trx1 maintains redox-active cysteines of Ref1 as well as those in the DNA-binding regions of transcription factors in a reduced state. Methods have been developed for the parallel measurement of the redox sates of nuclear and cytoplasmic Trx1 by using a redox Western blot approach (60). Whereas redox signaling events have been shown to interact with nuclear and cytoplasmic Trx1 in a differential manner (20, 21), little is known about the effects of nuclear oxidative stress on the redox couple.

The other major nuclear redox system is dependent on GSH. GSH-dependent mechanisms have been implicated in the maintenance of cysteine residues on zinc-finger DNA binding motifs in a reduced and functional state, DNA synthesis, and protection of DNA against oxidative stress (11). The GSH-associated antioxidant proteins glutathione peroxidase, glutathione reductase, and glutathione *S*-transferase display compartmented responses to oxidant stress (5, 30, 34). Oxidized intracellular GSH/GSSG ratios have been shown to inhibit NF-κB activity in certain cell types (19), a process that may occur through *S*-glutathionylation of cysteines in the DNA binding site of NF-κB or other associated proteins (13, 46). Therefore, the relative sensitivity of the nuclear glutathione pool to nuclear oxidative stress has important implications for specificity in localized redox signaling.

Currently, limited methods are available for the selective and controlled modulation of the nuclear redox state without simultaneously oxidizing the entire cell. Certain DNA-modifying agents such as doxorubicin (Adriamycin) and cisplatin are thought to induce nuclear oxidative stress; however, Adriamycin also modifies mitochondrial DNA, and cisplatin is a cross-linking agent inducing significant nonoxidative changes in nuclei (26). To provide a model with more-selective nuclear localized oxidative stress, we targeted a hydrogen peroxide (H_2O_2)-generating enzyme, D-amino acid oxidase (DAAO), to the nucleus. DAAO is a FAD-dependent oxidase, which catalyzes the deamination of D-amino acids to their corresponding imino acid form with stoichiometric production of H_2O_2. Imino acids are rapidly converted to their corresponding 2-oxo acid and ammonia (NH_3) (Fig. 1) (41). The use of

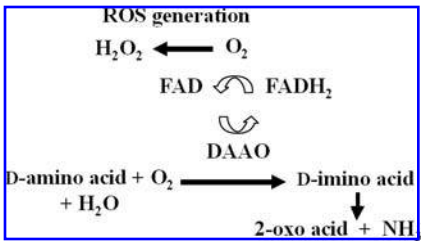

FIG. 1. Mechanism of ROS generation by D-amino acid oxidase. Oxidative deamination of D-amino acid to D-imino acid requires the participation of FAD cofactor. FAD is reduced during this half-reaction and is reoxidized by molecular oxygen (O_2), generating hydrogen peroxide (H_2O_2) to complete the reaction cycle. D-Imino acids spontaneously hydrolyze to 2-oxo acid and ammonia (NH_3) in solution.

nuclear-targeted DAAO offers several potential advantages as a tool for the study of redox-dependent nuclear systems such as transcription factor activity. Endogenous DAAO is present in peroxisomes, an organelle with high catalase activity. Previous research has shown that H_2O_2 generated in peroxisomes is preferentially metabolized in peroxisomes (29). Thus, even though endogenous DAAO produces H_2O_2 in response to added substrate, production of H_2O_2 by ectopic nuclear DAAO can be expected to introduce a selective nuclear oxidative stress. Furthermore, comparison to vector controls can be used to distinguish between effects of endogenous and ectopic DAAO (27). The vast majority of amino acids in eukaryotic organisms occur as the L-stereoisomer. Because of the enzyme specificities and mechanisms, D-amino acids are unlikely to affect other oxidase systems in the nucleus, such as lysyl oxidase, spermine oxidase, and NADPH oxidase 4 (32, 33). We describe a model for nuclear-specific oxidation by using nuclear-targeted DAAO. The system generates significant amounts of ROS, which are capable of interacting with nuclear redox machinery. The results show a preferential oxidation of nuclear GSH and an inhibition of NF-κB activity in the absence of nuclear Trx1 oxidation.

MATERIALS AND METHODS

Cloning of NLS-DAAO

Human D-amino acid oxidase cDNA expressed in pCMV6-XL5 was obtained from Origene, Rockville, MD. The cDNA was cloned into a nuclear-targeting vector, pCMV/Myc/nuc (Invitrogen, Carlsbad, CA) by polymerase chain reaction (PCR) between NcoI and XhoI restriction sites of the multiple cloning site. The forward and reverse primer sequences were 5′-CGACACCATGGCAATGCGTGTGGTG-3′ and 5′-ATCTACTCGAGGAGGT GGGATGGTGG-3′, respectively. Cloning was confirmed by running the digested product on an agarose gel and by direct sequencing.

Cell culture and transfection conditions

HeLa cells (ATCC, Manassas, VA), maintained in MEM (Minimum Essential Medium) supplemented with 10% fetal bovine serum and antibiotics (penicillin, streptomycin) were used for all experiments. Cells were transfected at 70–80% confluence by using the FuGENE 6 non–liposome-based system (Roche Applied Science, Indianapolis, IN). Fugene 6/DNA complexes were prepared by mixing Fugene 6 and DNA in a 3:1 ratio in serum-free MEM; 3 μl Fugene 6 to 1 μg DNA per plasmid per well for a six-well plate. Within individual experiments, all cells were transfected with equal amounts of DNA. Relative amounts of Fugene 6 and plasmid DNA were increased proportionately for transfection of 6-cm and 10-cm plates. All cells were transfected for 24 h with either pLacZ (Invitrogen) or NLS-DAAO in antibiotic-free MEM containing 10% FBS.

Western blotting and immunoprecipitation

Culture media were aspirated, and cells were washed once in PBS and collected in lysis buffer [20 m*M* HEPES, pH 7.8, 350 m*M* KCl, 1 m*M* $MgCl_2$, 0.5 m*M* EDTA, 0.1 m*M* EGTA,

1% vol/vol NP-40 with protease inhibitor tablet (Roche Applied Science) added fresh]. Protein lysates (30 μg) were separated on 10% SDS-PAGE, transferred to nitrocellulose membranes and probed for c-*Myc* (Sigma-Aldrich, St. Louis, MO). For p50 Western blots, nuclear and cytoplasmic fractions were obtained as described for Trx1 redox Western blotting. Nuclear extracts (15 μg) were separated on 10% SDS-PAGE, transferred to nitrocellulose membranes, and probed with anti-p50 (1:500) (Santa Cruz Biotechnology, Santa Cruz, CA). For immunoprecipitation of c-*Myc*–tagged proteins, cell lysates were incubated with monoclonal anti-c-*Myc* (1:1,000) for 1 h at 4°C and combined with protein-G agarose beads (2 h at 4°C) in accordance with manufacturer's guidelines (Sigma-Aldrich). Immunoprecipitated proteins were separated on 10% SDS-PAGE, transferred to nitrocellulose membrane, and probed with anti-DAAO (1:10,000) (Rockland Immunochemicals, Inc., Gilbertsville, PA).

Immunostaining

To confirm nuclear localization of NLS-DAAO, transfected cells were grown on coverslips and transfected as described earlier. Cells were fixed in –20°C methanol (10 min) and –20°C acetone (1 min), washed twice in PBS, and incubated with monoclonal anti-c-*Myc* (1:100) (Sigma-Aldrich) in PBS containing 1% BSA. Coverslips were washed 3 times in PBS, incubated with FITC-conjugated anti-mouse secondary antibody (1:1,000) (Invitrogen), washed 3 times in PBS, and placed on glass slides by using DAPI-containing mounting media (Vector Laboratories, Burlingame, CA). Slides were examined under a fluorescent microscope (Olympus BX61, Olympus, Center Valley, PA) with FITC and DAPI filters.

Measurement of ROS and cell viability

H_2O_2 generation by NLS-DAAO was measured with dichlorofluorescin diacetate (DCFH-DA) (Invitrogen). Cells (96-well plate, 10^4 per well) were loaded with dichlorofluorescin diacetate (DCFH-DA) (100 μ*M*) and incubated at 37°C for 30 min. Cells were treated with *N*-acetyl-D-alanine (NADA), *N*-acetyl-L-alanine (NALA) or H_2O_2, and fluorescence was measured at 1-min intervals over 30 min by using a fluorescence plate reader (SpectraMax M2, Molecular Devices, Sunnyvale, CA) with excitation at 485 nm and emission at 530 nm.

For analysis of cell viability, cells were plated in 24-well plates, transfected as described, and treated for 24 h with different concentrations of NADA or 1 m*M* H_2O_2. Cells were then incubated with methylthiazolyldiphenyltetrazolium bromide (MTT) reagent (Sigma-Aldrich) (5 mg/ml) for 2 h at 37°C, and the resulting formazan dye was solubilized in DMSO. Absorbance was measured at 550 nm.

Live cell thiol staining by CMF-DA

Cells were treated with NADA or H_2O_2 for 15 min, washed twice in PBS, and loaded with 5-chloromethylfluorescein-diacetate (CMF-DA) (Invitrogen) (4 μ*M*) in 1x PBS. Cells were incubated at 37°C for 15 min, washed with 1x PBS for 15 min at 37°C, and viewed under a fluorescent microscope (Olympus BX61) at 20x magnification with a fluorescein isothiocyanate (FITC) filter.

Trx1 redox Western blotting

For nuclear isolation, cells were scraped in 10 m*M* HEPES, pH 7.8, 10 m*M* KCl, 2 m*M* $MgCl_2$, 0.1 m*M* EDTA, 0.2 m*M* NaF, 0.2 m*M* $Na_3VO_4.6H_2O$ with protease inhibitor tablet, and iodoacetic acid (IAA) (50 m*M*) (59). Cell suspensions were incubated on ice for 5 min followed by Nonidet NP-40 treatment (final concentration, 0.6% vol/vol). After centrifugation at 16,000 *g*, the nuclear pellet and the cytosolic supernatant were separated and analyzed by redox Western blotting as follows. Subcellular fractions were treated with 6 *M* guanidine-HCl, 50 m*M* Tris, pH 8.3, 3 m*M* EDTA, and 0.5% Triton X-100 supplemented with 50 m*M* IAA (Sigma-Aldrich). Nuclear and cytoplasmic fractions showed minimal cross-contamination as measured by marker proteins (59). After 30 min at 37°C, the excess IAA was removed (Microspin G-25 columns; Amersham Biosciences Piscataway, NJ), and redox forms of Trx1 were separated by native polyacrylamide gel electrophoresis (60). The gel was electroblotted to nitrocellulose membrane and probed with goat anti-human Trx1 antibody (1:5,000) (American Diagnostica, Stamford, CT, U.S.A.). Membranes were then probed with an Alexafluor 680 anti-goat secondary antibody (1:5,000) (Invitrogen). Bands corresponding to Trx1 were visualized by using the Odyssey scanner (LI-COR, Lincoln, NE).

NF-κB reporter activity assay

NLS-DAAO–transfected cells were cotransfected with NF-κB luciferase reporter plasmid (Invitrogen) and pLacZ. For activation of NF-κB, cells were transiently exposed to exogenously added tumor necrosis factor-α (TNF-α) (10 ng/ml) or NADA (1 m*M*). After 1 h, TNF-α-containing media was aspirated and replaced with normal culture medium or NADA-containing media and incubated at 37°C for 7 h. Cells were then washed once with PBS and harvested in 1x reporter lysis buffer (Promega, Madison, WI). Luciferase assay reagent (Promega) was added to lysates, and luminescence was measured on a luminometer (Lumicount; GMI, Ramsey, MN). The effect of NADA (1 m*M*) on NF-κB luciferase reporter activity in TNF-α–stimulated cells was found to be minimal (data not shown). NF-κB luciferase reporter activity was normalized to β-galactosidase activity. 2-Nitrophenyl-β-D-galactopyranoside (ONPG) (Sigma-Aldrich) containing assay reagent was added to lysates. After incubation at 37°C for 15 min, absorbance was measured at 420 nm.

Measurement of subcellular protein S-*glutathionylation*

Nuclei and cytosol were isolated as described earlier for Trx1 redox Western blot, treated with ice-cold 100% trichloroacetic acid (TCA) [1:4 (vol/vol)], incubated at 4°C, and centrifuged to precipitate proteins. Protein pellets were washed with TCA and resuspended in 0.1 *M* NaOH to neutralize the acid and resolubilize the protein. Samples were reduced by treating with 5 m*M* DTT [1:1 (vol/vol)] at pH 8.0 for 30 min. After reduction, proteins were reprecipitated with cold 10% PCA/boric acid containing γ-glutamylglutamate as an internal standard, centrifuged, and GSH and GSSG in the

supernatant were measured by HPLC as *S*-carboxymethyl, *N*-dansyl derivatives as described (28).

Statistics

All the experiments were done at least 3 times with similar results, and representative figures are shown. Data were collected and expressed as mean ± SEM. Variation between groups was evaluated by one-way ANOVA, and *post hoc* significance tests were performed by using a Student's *t* test. A value of $p < 0.05$ was considered significant.

RESULTS

Expression and localization of NLS-DAAO

To determine expression levels and to verify the localization of nuclear- targeted D-amino acid oxidase (NLS-DAAO), HeLa cells were transfected with NLS-DAAO vector and analyzed by Western blot analysis at 24 h. Control cells were transfected with a LacZ-containing plasmid, which was used to determine transfection efficiency. Immunodetection of c-*Myc*–tagged NLS-DAAO revealed the presence of a single protein band in transfected cells whose weight corresponded to the theoretic weight of the tagged DAAO (42 kDa) (Fig. 2A). This 42-kDa protein was confirmed to be DAAO by immunoprecipitation with anti–c-*Myc* from whole-cell lysates and subsequent Western blot analysis with immunodetection of DAAO using anti-DAAO (Fig. 2A).

Previous studies show that DAAO occurs in several human tissues including liver, kidney, and brain, but is not uniformly distributed (42). Western blot analysis of HeLa cell lysates did not reveal detectable levels of endogenous DAAO (not shown). Immunofluorescence microscopy was used to determine subcellular localization of NLS-DAAO. Colocalization of c-*Myc* epitope tag (green) and the nuclear-specific dye, DAPI (blue), was observed in NLS-DAAO–transfected cells (Fig. 2B). No cytoplasmic localization of NLS-DAAO was observed. Furthermore, the absence of punctuate distribution in the cytoplasm indicates that the nuclear localization sequence of NLS-DAAO, which contains three tandem NLS sequences, supersedes intrinsic DAAO localization sequences that would otherwise target the protein to peroxisomes.

Effects of NLS-DAAO on ROS production, nuclear thiol oxidation, and cell viability

DAAO acts with greater efficiency on amino acids that have hydrophobic side chains, and D-alanine is a good substrate. However, preliminary experiments showed that *N*-acetylated D-alanine had greater activity in cells, presumably because this form has greater membrane permeability. Consequently, *N*-acetyl-D-alanine (NADA) was used as a substrate for DAAO to test for stimulation of H_2O_2. Hydrogen peroxide (H_2O_2) is a product of the oxidative deamination of D-amino acids, catalyzed by DAAO. The activity of NLS-DAAO in cells was indirectly monitored by measuring increased fluorescence due to oxidation of dichlorofluorescin diacetate (DCFH-DA). In the absence of NADA, DCF fluorescence did not increase in NLS-DAAO–transfected cells compared with transfection controls (Fig. 3A). A twofold increase in DCF fluorescence occurred at concentrations of 0.1 and 1 m*M* NADA. This extent of increase was less than the oxidation observed with 0.5 m*M* H_2O_2–treated positive controls, although no legitimate comparisons can be made between bolus addition of H_2O_2 to observed changes in steady-state H_2O_2 generation by the NLS-DAAO/NADA system. At less than the established K_m of DAAO for D-alanine (1.3 m*M*) (42), both 0.1 and 1 m*M* NADA, showed significant H_2O_2 generation in transfected cells. The 10 μ*M* NADA did not cause a significant increase in H_2O_2 production. When *N*-acetyl-L-alanine (NALA) was used in place of NADA, DCF fluorescence did not increase relative to untreated controls (Fig. 3A), thus establishing the stereospecificity of NLS-DAAO, and the apparent absence of production of H_2O_2 that could occur if racemases rapidly converted NALA to NADA. It must also be noted that ammonia and pyruvate, products of the NLS-DAAO–catalyzed oxidative deamination of NADA, can potentially alter the nuclear redox environment. Decreases in glutathione peroxidase, superoxide dismutase, and catalase activities and increases in superoxide production in submitochondrial particles are associated with ammonia-induced toxicity (31). Pyruvate has been shown to have a protective effect against H_2O_2-induced toxicity (39), thus acting in opposition to NLS-DAAO–derived H_2O_2. However, the demonstration of significant H_2O_2 generation in NLS-DAAO–transfected, NADA-treated versus pLacZ-transfected untreated cells (Fig. 3A) suggests that the effects of pyruvate and ammonia are minimal.

To test for nuclear-localized oxidation in NLS-DAAO–transfected cells, a thiol-specific fluorescent dye, 5-chloromethylfluorescein diacetate (CMF-DA) was used (Fig. 3B). CMF-DA binds principally to reduced GSH in what is thought to be a glutathione *S*-transferase–catalyzed reaction (56). CMF-DA binds to protein thiols with much lower affinity (47). Addition of 0.1 m*M* NADA to NLS-DAAO–transfected cells was sufficient to cause a significant decrease in nuclear thiol staining relative to control cells (Fig. 3B; NSL-DAAO, 0.1 m*M* NADA). The addition of substrate to control cells did not cause a change in nuclear thiol staining (Fig 3B; pLacZ, 0.1 m*M* NADA). Similarly, expression of NLS-DAAO in the absence of substrate did not affect the nuclear thiol pool (Fig. 3B; pLacZ, untreated). Untreated cells showed more intense nuclear thiol staining relative to the cytoplasm, thereby implying that the nuclear redox environment is more reducing than that of the cytoplasm. This is in general agreement with previous studies of compartmental redox state with CMF-DA (58). The absence of an increase in cytoplasmic thiol staining in NLS-DAAO–transfected, NADA-treated cells suggests nuclear-specific oxidation of GSH/GSSG rather than export of GSH into the cytoplasm.

The effect of NLS-DAAO–induced ROS on cell viability was examined by MTT assay (Fig. 3C). Cells were transfected for 24 h and treated for an additional 24 h with NADA to stimulate H_2O_2 production. A small but nonsignificant decrease in viability was seen in NADA-treated, NLS-DAAO–transfected cells compared with pLacZ-transfected, NADA-treated cells. In contrast, peroxide-treated cells showed almost complete loss of viability. The data suggest that H_2O_2 generation in response to NLS-DAAO does not

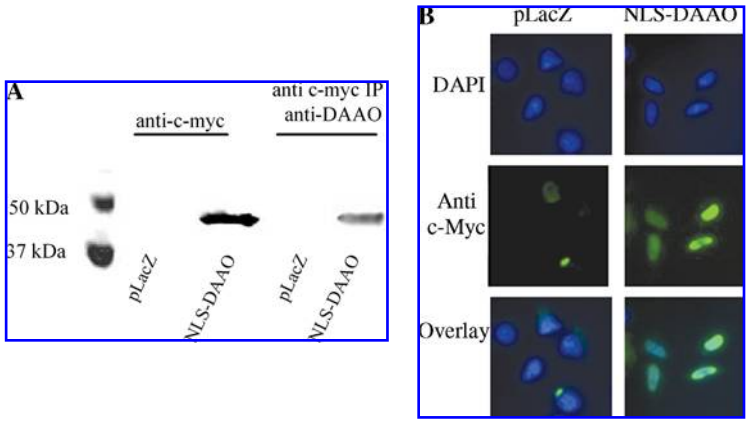

FIG. 2. Expression and localization of NLS-DAAO. (**A**) HeLa cells were transfected with either pLacZ (lanes 1, 3) or NLS-DAAO (lanes 2, 4), and lysates were run on 10% SDS-PAGE and immunoblotted with anti-c-*Myc* (lanes 1, 2). Additionally, c-*Myc*–tagged proteins were immunoprecipitated and immunoblotted with anti-DAAO (lanes 3, 4). (**B**) pLacZ and NLS-DAAO–transfected HeLa were fixed, incubated with anti–c-*Myc* primary antibody, co-stained with FITC-conjugated anti-mouse secondary antibody and DAPI, and viewed under a fluorescence microscope at 40x magnification.

cause an immediate cell death. Thus, the observed changes in thiols are not due to increased cell death.

Effects of NLS-DAAO on nuclear protein S*-glutathionylation*

The ability to measure nuclear GSH/GSSG redox state is hindered by loss of GSH from the nuclei during fractionation procedures. Previous estimates of nuclear GSH have given contradictory results (4, 7, 58). Here we examined the effects of NLS-DAAO–induced ROS on the nuclear GSH pool by measuring changes in the amount of nuclear *S*-glutathionylated protein (Pr-SSG) in transfected cells. Pr-SSG can form from reaction of GSSG with protein thiols (PrSH) or reaction of oxidized proteins with GSH. Content of Pr-SSG in nuclear and cytoplasmic components can be determined by measurement

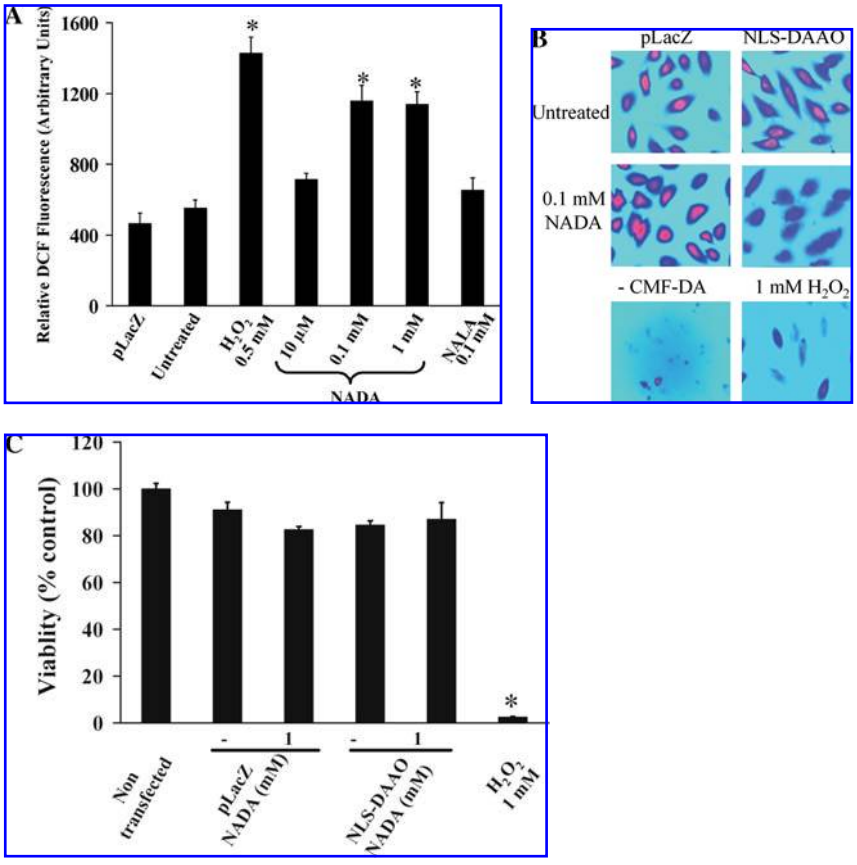

FIG. 3. Effects of NLS-DAAO on ROS production, thiol oxidation, and cell viability. (**A**) H_2O_2 production in NLS-DAAO–transfected cells treated with *N*-acetyl-D-alanine (NADA), *N*-acetyl-L-alanine (NALA) or H_2O_2 for 10 min was measured by fluorescence due to dichlorofluorescin diacetate (DCFH-DA) oxidation. Each data point represents the mean ± SEM; $n = 4$. *Significantly different relative to NLS-DAAO–transfected, untreated control, $p < 0.05$ (one-way ANOVA and *post hoc* Student's *t* test for significance). (**B**) NLS-DAAO– and pLacZ-transfected cells were treated with or without NADA (*top four panels*) for 10 min, and nontransfected cells were treated with H_2O_2 for 10 min (*bottom right*). Cells were stained with the thiol binding dye, 5-chloromethylfluorescein (CMF-DA), and viewed under a fluorescence microscope. The resulting green fluorescence images were converted to pseudocolor, with pink areas representing higher intensities and blue representing lower intensities. Unstained cells were not visible (*bottom left*). (**C**) Cell viability. pLacZ- and NLS-DAAO–transfected cells were treated with or without NADA; cell viability was assayed by the MTT assay, carried out as described in Methods and Methods. Viabilities (mean ± SEM; $n = 4$; *significantly different relative to nontransfected, untreated control, $p < 0.05$, one-way ANOVA with *post hoc* Student's *t* test for significance) are expressed as a percentage of nontransfected, untreated controls.

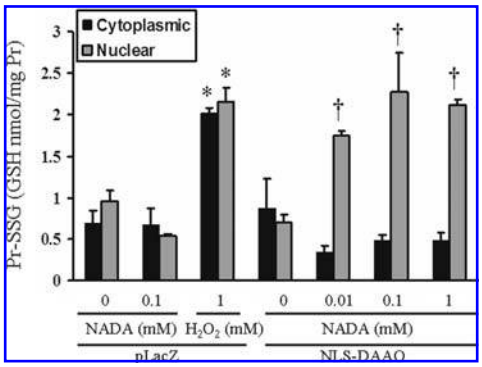

FIG. 4. Nuclear and cytoplasmic protein *S*-glutathionylation in NLS-DAAO–transfected cells. Cells were transfected and treated with different concentrations of NADA or H_2O_2 for 10 min as shown. Nuclear and cytoplasmic fractions were obtained as described in Materials and Methods. Proteins were precipitated in trichloroacetic acid, and protein-bound GSH was extracted from nuclear and cytoplasmic protein fractions by reduction with DTT and measured by HPLC. The Y-axis represents GSH derived from glutathionylated protein (Pr-SSG) normalized to total protein amounts. Data points represent the mean ± SEM; $n = 3$; *significantly different relative to pLacZ, untreated control, †significantly different relative to NLS-DAAO–transfected, untreated control, $p < 0.05$, one-way ANOVA with *post hoc* Student's *t* test for significance.

of released GSH by HPLC, after reduction of nuclear and cytoplasmic protein fractions with DTT (15) (Fig. 4). In pLacZ-transfected, untreated cells, cytoplasmic and nuclear Pr-SSG–derived GSH were 0.68 ± 0.15 and 0.96 ± 0.12 nmol/mg Pr, respectively (Fig. 4; pLacZ-transfected). H_2O_2-treated (1 m*M*) cells showed significant increases in both cytoplasmic and nuclear Pr-SSG . In NLS-DAAO–transfected, untreated cells, cytoplasmic and nuclear Pr-SSG–derived GSH values were 0.87 ± 0.35 and 0.7 ± 0.1 nmol/mg Pr, respectively (Fig. 4; NLS-DAAO–transfected, untreated). In NLS-DAAO–transfected, NADA-treated cells, cytoplasmic and nuclear Pr-SSG– derived GSH values were 0.34 ± 0.08 to 0.48 ± 0.09 nmol/mg Pr and 1.75 ± 0.23 to 2.2 ± 0.22 nmol/mg Pr, respectively (Fig. 4, NLS-DAAO–transfected). This represents a twofold increase in Pr-SSG in the nucleus induced by NLS-DAAO. Decreases in cytoplasmic Pr-SSG in NLS-DAAO–transfected/untreated versus NLS-DAAO–transfected/NADA treated were not found to be significant. These concentrations of Pr-SSG–derived GSH represent only a small fraction (<5%) of total cellular GSH/GSSG (data not shown). Interestingly, substantial oxidation in nuclear glutathione occurred with the addition of 0.01, 0.1, or 1 m*M* NADA, although the data do not support a NADA concentration-dependent response. Variations in transfection efficiency, substrate delivery, and glutaredoxin activity may account for this observation. Significant ROS generation was not detected by DCF oxidation in NLS-DAAO–transfected, 0.01 m*M* NADA-treated cells (Fig. 3A), even though nuclear Pr-SSG did increase under these conditions, suggesting that nuclear GSH/GSSG is highly sensitive to NLS-DAAO–induced oxidative stress, scavenging ROS and preventing detection by DCF.

Effects of NLS-DAAO on Trx1 redox state

Changes in Trx1 redox state in NLS-DAAO–transfected cells were examined by redox Western analysis with cell fractionation, to provide redox state in both cytoplasmic and nuclear compartments (Fig. 5). Cells were transfected for 24 h and subsequently treated with 1 m*M* NADA for ≤30 min (Fig. 5A). No oxidation of nuclear Trx1 was seen in NLS-DAAO–transfected, NADA-treated cells at any of the time points examined relative to untreated, pLacZ-transfected cells (Fig. 5A, B). Likewise, treatment with 1 m*M* NADA in the absence of NLS-DAAO did not cause oxidation of nuclear Trx1 (Fig. 5B). No differences in Trx1 redox state between NLS-DAAO–transfected and control cells were observed in cytoplasmic fractions. Nuclear and cytoplasmic Trx1 redox state did not change at 12 or 24 h after NADA treatment (data not shown). Significant oxidation of Trx1 occurred in both nuclear and cytoplasmic fractions in H_2O_2-treated cells (Fig. 5B). Similarly, DTT-treated cells showed significant reduction of Trx1 in both subcellular fractions (Fig. 5B).

NF-κB activity in NLS-DAAO–transfected cells

The role of subcellular compartmentation in the regulation of the redox-sensitive transcription factor, NF-κB, has been well established. Here we tested the ability of nuclear-localized oxidative stress to influence NF-κB activity. With a known stimulator of NF-κB activity, tumor necrosis factor-α (TNF-α) (44), we first examined the effect of NLS-DAAO/NADA on TNF-α–induced nuclear translocation of the NF-κB subunit, p50. Western blot analysis of p50 nuclear fractions (normalized

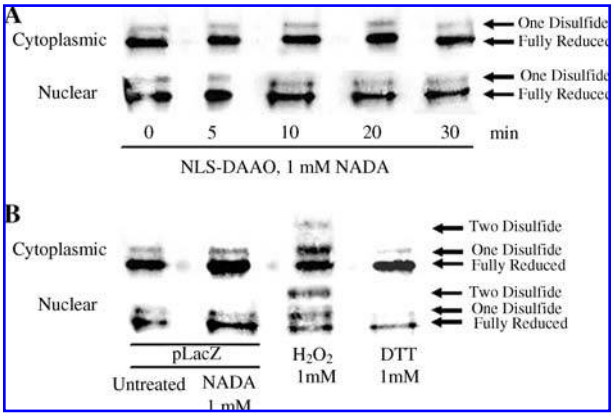

FIG. 5. Nuclear and cytoplasmic Trx1 redox states in NLS-DAAO–transfected cells. (**A**) Cells were transfected with NLS-DAAO and treated with 1 m*M* NADA for 0–30 min as indicated. Redox Western analysis of cytoplasmic (top) and nuclear (bottom) Trx1 was carried out as described in Materials and Methods. (**B**) Cells were transfected with pLacZ (lanes 1, 2) or nontransfected (lanes 3, 4) and treated as indicated for 10 min. Carboxymethylated Trx1 appears as three distinct bands: top band is the two disulfide form, present under highly oxidizing conditions (H_2O_2-treated, **B**, lane 3), middle band is the one disulfide-oxidized form (principally active-site oxidation), and the lower band is the fully reduced form (60). The experiment shown is representative of results obtained from four separate experiments.

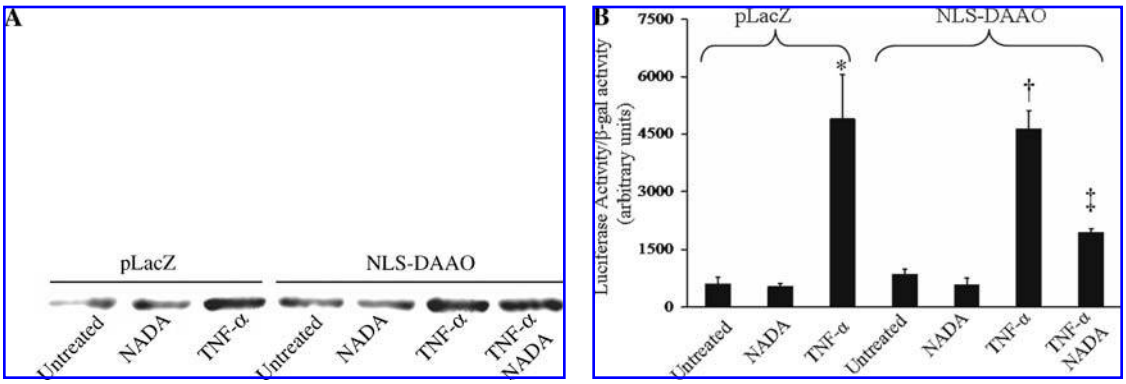

FIG. 6. The effects of nuclear-localized oxidative stress on NF-κB nuclear translocation and NF-κB reporter activity. (**A**) Cells were cotransfected with pLacZ or NLS-DAAO and treated with NADA (1 m*M*) or TNF-α (10 ng/ml) for 1 h. Nuclear protein extracts (15 μg per lane) were separated by 10% SDS-PAGE and probed with anti-p50. (**B)** Cells were cotransfected with NLS-DAAO, NF-κB reporter plasmid and pLacZ and NF-κB was stimulated with TNF-α (10 ng/ml) for 1 h. TNF-α–containing media was removed, and cells were incubated in normal or NADA (1 m*M*)-containing media for 7 h. Luminescence values were normalized to corresponding β-galactosidase activities for each sample. Data points represent the mean ± SEM; $n = 3$; *significantly different relative to pLacZ-transfected, untreated control; †significantly different relative to NLS-DAAO–transfected, untreated control; ‡significantly different relative to NLS-DAAO–transfected, TNF-α–treated control; $p < 0.05$, one-way ANOVA with *post hoc* Student's *t* test for significance.

to protein amount) showed significant increases in p50 nuclear translocation in both pLacZ and NLS-DAAO–transfected cells after 1 h of TNF-α (10 ng/ml) stimulation (Fig. 6A). NADA treatment (1 m*M*, 1 h) of pLacZ and NLS-DAAO–transfected cells did not induce p50 nuclear translocation. TNF-α–induced p50 nuclear translocation was unaffected in NLS-DAAO–transfected, NADA-treated cells (Fig. 6A). Next, we investigated the effects of NLS-DAAO–induced ROS on NF-κB reporter activity. Cells were cotransfected with NLS-DAAO, NF-κB luciferase reporter, and pLacZ for 24 h. Luciferase activity was normalized to β-galactosidase activity (Fig. 6B). NF-κB activity was stimulated by a single addition of TNF-α (10 ng/ml, 1 h), and then followed up over 7 h. TNF-α caused a fivefold increase in NF-κB reporter expression relative to unstimulated control in pLacZ-transfected and NLS-DAAO–transfected cells. TNF-α–induced NF-κB reporter activity was significantly suppressed in NLS-DAAO–transfected, NADA-treated cells (58% decrease relative to NLS-DAAO–transfected, TNF-α–treated cells), suggesting that nuclear localized ROS had an inhibitory effect on NF-κB DNA binding activity.

DISCUSSION

The redox machinery of the nucleus and the systems it regulates represent a vital component of intracellular redox signaling pathways, integrating antioxidant response, control of gene transcription, and repair of oxidative DNA damage. We investigated the relative responsiveness of nuclear redox couples Trx1 and GSH/GSSG to nuclear-specific oxidative stress by using a H_2O_2-generating enzyme targeted to the nucleus. We further examined the capacity of this localized H_2O_2 generation for the inhibition of NF-κB–dependent transcription by using a reporter system. The results show that nuclear GSH/GSSG is more sensitive to subcellular oxidation than are nuclear Trx1 and that NF-κB, which contains a redox-sensitive cysteine in the DNA-binding region, and has decreased activity under conditions of nuclear oxidative stress.

Previous studies show a dual role for Trx1 in the regulation of NF-κB activation and DNA binding (24). In the cytoplasm, Trx1 has an inhibitory effect on I-κB kinase, thus inhibiting NF-κB translocation to the nucleus. In the nucleus, Trx1 promotes DNA binding of NF-κB by maintaining redox-active cysteines of p50 in a reduced state via its interaction with Ref1 (40, 43). Overexpression of nuclear Trx1 promotes DNA binding of p50 and redox modification of Cys62 in p50 results in decreased DNA binding (37, 38, 46). Although the compartmentation of redox regulation of NF-κB has been established, as well as the effects of extranuclear oxidative stress, the effects of nuclear-localized oxidative stress on this system are unclear. By using NLS-DAAO/NADA as a tool for H_2O_2 generation in the nucleus, we found that nuclear- specific oxidative stress causes the inhibition of NF-κB reporter activity in the absence of nuclear Trx1 oxidation. Whereas this finding does not exclude nuclear Trx1 as a major component in the redox regulation of NF-κB in the nucleus, it does suggest that nuclear-localized H_2O_2 interacts more readily with other nuclear redox-sensitive components that influence NF-κB activity. Possible sites of redox sensitivities are shown schematically in Fig. 7. Inhibition of NF-κB activity by NLS-DAAO– induced nuclear oxidative stress may be caused by oxidation of Ref1 (arrow 1, Fig. 7) or by direct oxidative modification of redox-active cysteines in the DNA binding site of p50, as described later (arrows 2–4, Fig. 7).

In vitro models reveal that *S*-glutathionylation of Cys62 reversibly inhibits DNA binding of the transcription factor (46). Similarly, artificially shifting the GSH/GSSG redox balance in cultured cells by the addition of *N*-acetyl cysteine (NAC) promotes NF-κB activation (19). Given the significant increase in

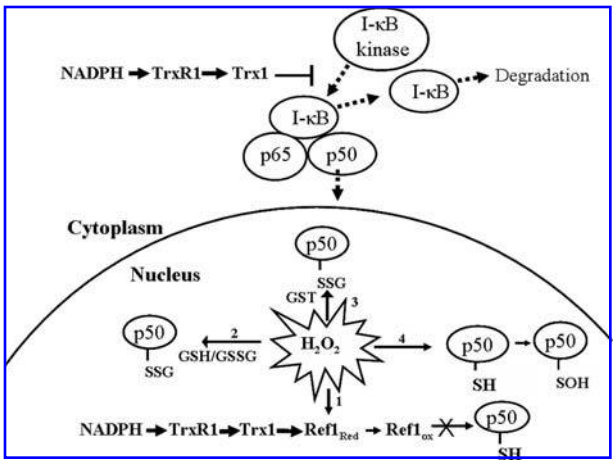

FIG. 7. Scheme of nuclear oxidative stress-induced inhibition of NF-κB activity. NF-κB translocates from the cytoplasm to the nucleus when it becomes unbound from I-κB, a process regulated by Trx1-dependent control of I-κB kinase. Nuclear-localized H_2O_2 inhibits NF-κB activity, potentially through modulation of p50 redox-active cysteine in the DNA-binding region. Mechanistically, this may occur by (1) oxidation of Ref1, thereby preventing it from maintaining p50 in a reduced state, (2) *S*-glutathionylation of p50 by GSSG nonenzymatically or catalyzed by glutaredoxin-1, (3) GST-mediated glutathionylation of p50, or (4) direct oxidation of p50 redox-active cysteine, yielding sulphenic acid.

nuclear Pr-SSG observed here, it is possible that *S*-glutathionylation of p50 forms the mechanistic basis for the inhibition of NF-κB activity during nuclear oxidative stress (arrow 2, Fig. 7). Protein *S*-glutathionylation has been proposed to occur by GSSG reacting directly with protein thiols (14) or by GSH reacting with activated thiol residues (8). The former may be limited by the low concentrations of GSSG (micromolar range) in the cell. Here we observed protein *S*-glutathionylation within 15 min of treatment with NADA, which may indicate a substantial oxidation of the nuclear GSH/GSSG pool, resulting in significant Pr-SSG formation. Alternatively, oxidative modification of Cys62 in p50 may occur through formation of sulphenic acid (–SOH) (arrow 4, Fig. 7) (46).

Preferential GSH/GSSG oxidation appears to point to protein *S*-glutathionylation as an important mechanism by which the nuclear redox environment adapts to oxidative challenge. *S*-Glutathionylation as a signaling mechanism is advantageous, as it is reversible, can occur rapidly due to catalysis by glutaredoxin-1, and can be highly specific (12, 54). Previous studies show that H_2O_2, generated in cells at subtoxic levels by the addition of glucose oxidase, causes protein *S*-glutathionylation, although not at the same levels elicited by exogenous oxidant (9). Others have demonstrated correlations between *S*-glutathionylation and gene expression during oxidative stress (13). Interestingly, genes involved in NF-κB activation and DNA methylation were overrepresented among genes most responsive to GSH depletion. This suggests that nuclear-specific proteins may be particularly responsive to *S*-glutathionylation. *S*-Glutathionylation can also result in altered enzymatic activity (18, 36). We have demonstrated a significant increase in nuclear protein *S*-glutathionylation in response to subtoxic levels of H_2O_2 in the nucleus. Because cytoplasmic Pr-SSG is not affected under these conditions, we conclude that a localized set of nuclear proteins undergo *S*-glutathionylation as part of the nuclear oxidative stress response. It has yet to be determined what the critical nuclear proteins are in this scheme, but redox-active proteins such as Ref1 and peroxiredoxins are likely targets, as *S*-glutathionylation could protect against irreversible oxidation.

Glutathione *S*-transferase (GST) may contribute to Pr-SSG formation in the context of nuclear oxidative stress. Although the role of GST in cell signaling in the cytoplasm through its interaction with apoptosis signal–regulating kinase 1 (ASK1) and c-Jun N-terminal kinase (JNK) has been established, its role in redox signaling in the nucleus is less clear (1, 6). Because of their drug-metabolizing ability, GSTs are frequently studied in terms of drug efficacy. Indeed, GST-pi has been found to be highly expressed in certain cancer cells (52), and increased GST-pi in the nucleus is associated, clinically, with more aggressive tumors (2, 17). Some anticancer drugs such as doxorubicin and cisplatin are thought to generate ROS as a cytotoxic byproduct (53). Additionally, GSH depletion is associated with decreased drug resistance, due to diminished efflux of the drug (3). Given the model described here of nuclear-localized ROS induced–Pr-SSG formation, it is possible that drug-induced ROS also causes an increase in Pr-SSG either through oxidation of GSH/GSSG or through alterations in GST-pi localization and activity (arrow 3, Fig. 7). Recent studies have revealed an association between GST-pi and the reactivation of oxidized 1-Cys Prx, further highlighting a potential role for nuclear-localized ROS in redox signaling (49).

In conclusion, the present results demonstrate that using a nuclear-targeted D-amino acid oxidase provides a model for specific nuclear oxidation. Under these conditions, nuclear GSH/GSSG, as measured by Pr-SSG, shows greater responsiveness than Trx1 to nuclear oxidative stress. The results, surprisingly, show that NF-κB reporter activity is inhibited even without oxidation of nuclear Trx1. Consequently, the data suggest a major role for nuclear protein *S*-glutathionylation in controlling nuclear transcription during nuclear oxidative stress.

ACKNOWLEDGMENT

This work was supported by National Institutes of Health (NIH) grant ES011195.

ABBREVIATIONS

ASK 1, apoptosis signal–regulating kinase 1; AP-1, activator protein 1; CMF-DA, 5-chloromethylfluoresein diacetate; DAA, D-amino acid; DAAO, D-amino acid oxidase; DCFH-DA, dichlorofluorescin diacetate; Gpx, glutathione peroxidase; GSH, reduced glutathione; GSSG, glutathione disulfide; GST, glutathione *S*-transferase; JNK, c-jun N-terminal kinase; NAC, *N*-acetyl cysteine; NADA,

N-acetyl-D-alanine, NF-κB, nuclear factor κB; Prx, peroxiredoxin; Pr-SSG, *S*-glutathionylated protein; ROS, reactive oxygen species; Trx1, thioredoxin 1; TNF-α, tumor necrosis factor-α.

REFERENCES

1. Adler V, Yin Z, Fuchs SY, Benezra M, Rosario L, Tew KD, Pincus MR, Sardana M, Henderson CJ, Wolf CR, Davis RJ, and Ronai Z. Regulation of JNK signaling by GSTp. *EMBO J* 18: 1321–1334, 1999.
2. Ali-Osman F, Brunner JM, Kutluk TM, and Hess K. Prognostic significance of glutathione *S*-transferase pi expression and subcellular localization in human gliomas. *Clin Cancer Res* 3: 2253–2261, 1997.
3. Batist G, Schecter R, Woo A, Greene D, and Lehnert S. Glutathione depletion in human and in rat multi-drug resistant breast cancer cell lines. *Biochem Pharmacol* 41: 631–635, 1991.
4. Bellomo G, Vairetti M, Stivala L, Mirabelli F, Richelmi P, and Orrenius S. Demonstration of nuclear compartmentalization of glutathione in hepatocytes. *Proc Natl Acad Sci U S A* 89: 4412–4416, 1992.
5. Borchert A, Savaskan NE, and Kuhn H. Regulation of expression of the phospholipid hydroperoxide/sperm nucleus glutathione peroxidase gene: tissue-specific expression pattern and identification of functional cis- and trans-regulatory elements. *J Biol Chem* 278: 2571–2580, 2003.
6. Cho SG, Lee YH, Park HS, Ryoo K, Kang KW, Park J, Eom SJ, Kim MJ, Chang TS, Choi SY, Shim J, Kim Y, Dong MS, Lee MJ, Kim SG, Ichijo H, and Choi EJ. Glutathione S-transferase mu modulates the stress-activated signals by suppressing apoptosis signal-regulating kinase 1. *J Biol Chem* 276: 12749–12755, 2001.
7. Cotgreave IA. Analytical developments in the assay of intra- and extracellular GSH homeostasis: specific protein S-glutathionylation, cellular GSH and mixed disulphide compartmentalisation and interstitial GSH redox balance. *Biofactors* 17: 269–277, 2003.
8. Dalle-Donne I, Rossi R, Giustarini D, Colombo R, and Milzani A. Actin S-glutathionylation: evidence against a thiol-disulphide exchange mechanism. *Free Radic Biol Med* 35: 1185–1193, 2003.
9. Dandrea T, Bajak E, Warngard L, and Cotgreave IA. Protein S-glutathionylation correlates to selective stress gene expression and cytoprotection. *Arch Biochem Biophys* 406: 241–252, 2002.
10. Denu JM and Tanner KG. Specific and reversible inactivation of protein tyrosine phosphatases by hydrogen peroxide: evidence for a sulfenic acid intermediate and implications for redox regulation. *Biochemistry* 37: 5633–5642, 1998.
11. Dickinson DA and Forman HJ. Glutathione in defense and signaling: lessons from a small thiol. *Ann N Y Acad Sci* 973: 488–504, 2002.
12. Fratelli M, Gianazza E, and Ghezzi P. Redox proteomics: identification and functional role of glutathionylated proteins. *Exp Rev Proteomics* 1: 365–376, 2004.
13. Fratelli M, Goodwin LO, Orom UA, Lombardi S, Tonelli R, Mengozzi M, and Ghezzi P. Gene expression profiling reveals a signaling role of glutathione in redox regulation. *Proc Natl Acad Sci U S A* 102: 13998–14003, 2005.
14. Gilbert HF. Thiol/disulfide exchange equilibria and disulfide bond stability. *Methods Enzymol* 251: 8–28, 1995.
15. Go YM, Ziegler TR, Johnson JM, Gu L, Hansen JM, and Jones DP. Selective protection of nuclear thioredoxin-1 and glutathione redox systems against oxidation during glucose and glutamine deficiency in human colonic epithelial cells *Free Radic Biol Med* 42: 363–370, 2007.
16. Goossens V, Grooten J, De Vos K, and Fiers W. Direct evidence for tumor necrosis factor-induced mitochondrial reactive oxygen intermediates and their involvement in cytotoxicity. *Proc Natl Acad Sci U S A* 92: 8115–8119, 1995.
17. Goto S, Ihara Y, Urata Y, Izumi S, Abe K, Koji T, and Kondo T. Doxorubicin-induced DNA intercalation and scavenging by nuclear glutathione S-transferase pi. *FASEB J* 15: 2702–2714, 2001.
18. Grant CM, Quinn KA, and Dawes IW. Differential protein S-thiolation of glyceraldehyde-3-phosphate dehydrogenase isoenzymes influences sensitivity to oxidative stress. *Mol Cell Biol* 19: 2650–2656, 1999.
19. Haddad JJ, Olver RE, and Land SC. Antioxidant/pro-oxidant equilibrium regulates HIF-1alpha and NF-kappa B redox sensitivity: evidence for inhibition by glutathione oxidation in alveolar epithelial cells. *J Biol Chem* 275: 21130–21139, 2000.
20. Halvey PJ, Watson WH, Hansen JM, Go YM, Samali A, and Jones DP. Compartmental oxidation of thiol-disulphide redox couples during epidermal growth factor signalling. *Biochem J* 386: 215–219, 2005.
21. Hansen JM, Watson WH, and Jones DP. Compartmentation of Nrf-2 redox control: regulation of cytoplasmic activation by glutathione and DNA binding by thioredoxin-1. *Toxicol Sci* 82: 308–317, 2004.
22. Hansen JM, Zhang H, and Jones DP. Mitochondrial thioredoxin-2 has a key role in determining tumor necrosis factor-alpha-induced reactive oxygen species generation, NF-kappaB activation, and apoptosis. *Toxicol Sci* 91: 643–650, 2006.
23. Hirota K, Matsui M, Iwata S, Nishiyama A, Mori K, and Yodoi J. AP-1 transcriptional activity is regulated by a direct association between thioredoxin and Ref-1. *Proc Natl Acad Sci U S A* 94: 3633–3638, 1997.
24. Hirota K, Murata M, Sachi Y, Nakamura H, Takeuchi J, Mori K, and Yodoi J. Distinct roles of thioredoxin in the cytoplasm and in the nucleus: a two-step mechanism of redox regulation of transcription factor NF-kappaB. *J Biol Chem* 274: 27891–27897, 1999.
25. Jayaraman L, Murthy KG, Zhu C, Curran T, Xanthoudakis S, and Prives C. Identification of redox/repair protein Ref-1 as a potent activator of p53. *Genes Dev* 11: 558–570, 1997.
26. Jevtovic-Todorovic V and Guenthner TM. Depletion of a discrete nuclear glutathione pool by oxidative stress, but not by buthionine sulfoximine: correlation with enhanced alkylating agent cytotoxicity to human melanoma cells in vitro. *Biochem Pharmacol* 44: 1383–1393, 1992.
27. Jones DP. Intracellular catalase function: analysis of the catalatic activity by product formation in isolated liver cells. *Arch Biochem Biophys* 214: 806–814, 1982.
28. Jones DP. Redox potential of GSH/GSSG couple: assay and biological significance. *Methods Enzymol* 348: 93–112, 2002.
29. Jones DP, Eklow L, Thor H, and Orrenius S. Metabolism of hydrogen peroxide in isolated hepatocytes: relative contributions of catalase and glutathione peroxidase in decomposition of endogenously generated H_2O_2. *Arch Biochem Biophys* 210: 505–516, 1981.
30. Kamada K, Goto S, Okunaga T, Ihara Y, Tsuji K, Kawai Y, Uchida K, Osawa T, Matsuo T, Nagata I, and Kondo T. Nuclear glutathione S-transferase pi prevents apoptosis by reducing the oxidative stress-induced formation of exocyclic DNA products. *Free Radic Biol Med* 37: 1875–1884, 2004.
31. Kosenko E, Kaminsky Y, Kaminsky A, Valencia M, Lee L, Hermenegildo C, and Felipo V. Superoxide production and antioxidant enzymes in ammonia intoxication in rats. *Free Radic Res* 27: 637–644, 1997.
32. Kuroda J, Nakagawa K, Yamasaki T, Nakamura K, Takeya R, Kuribayashi F, Imajoh-Ohmi S, Igarashi K, Shibata Y, Sueishi K, and Sumimoto H. The superoxide-producing NAD(P)H oxidase Nox4 in the nucleus of human vascular endothelial cells. *Genes Cells* 10: 1139–1151, 2005.
33. Li W, Nellaiappan K, Strassmaier T, Graham L, Thomas KM, and Kagan HM. Localization and activity of lysyl oxidase within nuclei of fibrogenic cells. *Proc Natl Acad Sci U S A* 94: 12817–12822, 1997.
34. Lundberg M, Johansson C, Chandra J, Enoksson M, Jacobsson G, Ljung J, Johansson M, and Holmgren A. Cloning and expression of a novel human glutaredoxin (Grx2) with mitochondrial and nuclear isoforms. *J Biol Chem* 276: 26269–26275, 2001.
35. Makino Y, Yoshikawa N, Okamoto K, Hirota K, Yodoi J, Makino I, and Tanaka H. Direct association with thioredoxin allows redox regulation of glucocorticoid receptor function. *J Biol Chem* 274: 3182–3188, 1999.
36. Mallis RJ, Hamann MJ, Zhao W, Zhang T, Hendrich S, and Thomas JA. Irreversible thiol oxidation in carbonic anhydrase, III:

protection by S-glutathiolation and detection in aging rats. *Biol Chem* 383: 649–662, 2002.
37. Marshall HE, and Stamler JS. Inhibition of NF-kappa B by S-nitrosylation. *Biochemistry* 40: 1688–1693, 2001.
38. Matthews JR, Kaszubska W, Turcatti G, Wells TN, and Hay RT. Role of cysteine62 in DNA recognition by the P50 subunit of NF-kappa B. *Nucleic Acids Res* 21: 1727–1734, 1993.
39. Mazzio E and Soliman KF. Pyruvic acid cytoprotection against 1-methyl-4-phenylpyridinium, 6-hydroxydopamine and hydrogen peroxide toxicities in vitro. *Neurosci Lett* 337: 77–80, 2003.
40. Mitomo K, Nakayama K, Fujimoto K, Sun X, Seki S, and Yamamoto K. Two different cellular redox systems regulate the DNA-binding activity of the p50 subunit of NF-kappa B in vitro. *Gene* 145: 197–203, 1994.
41. Molla G, Bernasconi M, Sacchi S, Pilone MS, and Pollegioni L. Expression in *Escherichia coli* and in vitro refolding of the human protein pLG72. *Protein Exp Purif* 46: 150–155, 2006.
42. Molla G, Sacchi S, Bernasconi M, Pilone MS, Fukui K, and Polegioni L. Characterization of human D-amino acid oxidase. *FEBS Lett* 580: 2358–2364, 2006.
43. Nishi T, Shimizu N, Hiramoto M, Sato I, Yamaguchi Y, Hasegawa M, Aizawa S, Tanaka H, Kataoka K, Watanabe H, and Handa H. Spatial redox regulation of a critical cysteine residue of NF-kappa B in vivo. *J Biol Chem* 277: 44548–44556, 2002.
44. Osborn L, Kunkel S, and Nabel GJ. Tumor necrosis factor alpha and interleukin 1 stimulate the human immunodeficiency virus enhancer by activation of the nuclear factor kappa B. *Proc Natl Acad Sci U S A* 86: 2336–2340, 1989.
45. Piette J, Piret B, Bonizzi G, Schoonbroodt S, Merville MP, Legrand-Poels S, and Bours V. Multiple redox regulation in NF-kappaB transcription factor activation. *Biol Chem* 378: 1237–1245, 1997.
46. Pineda-Molina E, Klatt P, Vazquez J, Marina A, Garcia de Lacoba M, Perez-Sala D, and Lamas S. Glutathionylation of the p50 subunit of NF-kappaB: a mechanism for redox-induced inhibition of DNA binding. *Biochemistry* 40: 14134–14142, 2001.
47. Poot M, Kavanagh TJ, Kang HC, Haugland RP, and Rabinovitch PS. Flow cytometric analysis of cell cycle-dependent changes in cell thiol level by combining a new laser dye with Hoechst 33342. *Cytometry* 12: 184–187, 1991.
48. Powis G and Montfort WR. Properties and biological activities of thioredoxins. *Annu Rev Biophys Biomol Struct* 30: 421–455, 2001.
49. Ralat LA, Manevich Y, Fisher AB, and Colman RF. Direct evidence for the formation of a complex between 1-cysteine peroxiredoxin and glutathione S-transferase pi with activity changes in both enzymes. *Biochemistry* 45: 360–372, 2006.
50. Reynaert NL, Ckless K, Korn SH, Vos N, Guala AS, Wouters EF, van der Vliet A, and Janssen-Heininger YM. Nitric oxide represses inhibitory kappaB kinase through S-nitrosylation. *Proc Natl Acad Sci U S A* 101: 8945–8950, 2004.
51. Saitoh M, Nishitoh H, Fujii M, Takeda K, Tobiume K, Sawada Y, Kawabata M, Miyazono K, and Ichijo H. Mammalian thioredoxin is a direct inhibitor of apoptosis signal-regulating kinase (ASK) 1. *EMBO J* 17: 2596–2606, 1998.
52. Shiratori Y, Hada Y, Maruyama H, Shinagawa S, and Tateoka N. [Immunohistochemical and biochemical investigations on glutathione S-transferases in the human placenta]. *Nippon Sanka Fujinka Gakkai Zasshi* 39: 547–552, 1987.
53. Sinha BK and Mimnaugh EG. Free radicals and anticancer drug resistance: oxygen free radicals in the mechanisms of drug cytotoxicity and resistance by certain tumors. *Free Radic Biol Med* 8: 567–581, 1990.
54. Starke DW, Chock PB, and Mieyal JJ. Glutathione-thiyl radical scavenging and transferase properties of human glutaredoxin (thioltransferase): potential role in redox signal transduction. *J Biol Chem* 278: 14607–14613, 2003.
55. Sundaresan M, Yu ZX, Ferrans VJ, Irani K, and Finkel T. Requirement for generation of H_2O_2 for platelet-derived growth factor signal transduction. *Science* 270: 296–299, 1995.
56. Tauskela JS, Hewitt K, Kang LP, Comas T, Gendron T, Hakim A, Hogan M, Durkin J, and Morley P. Evaluation of glutathione-sensitive fluorescent dyes in cortical culture. *Glia* 30: 329–341, 2000.
57. Toledano MB and Leonard WJ. Modulation of transcription factor NF-kappa B binding activity by oxidation-reduction in vitro. *Proc Natl Acad Sci U S A* 88: 4328–4332, 1991.
58. Voehringer DW, McConkey DJ, McDonnell TJ, Brisbay S, and Meyn RE. Bcl-2 expression causes redistribution of glutathione to the nucleus. *Proc Natl Acad Sci U S A* 95: 2956–2960, 1998.
59. Watson WH and Jones DP. Oxidation of nuclear thioredoxin during oxidative stress. *FEBS Lett* 543: 144–147, 2003.
60. Watson WH, Pohl J, Montfort WR, Stuchlik O, Reed MS, Powis G, and Jones DP. Redox potential of human thioredoxin 1 and identification of a second dithiol/disulfide motif. *J Biol Chem* 278: 33408–33415, 2003.
61. Wei SJ, Botero A, Hirota K, Bradbury CM, Markovina S, Laszlo A, Spitz DR, Goswami PC, Yodoi J, and Gius D. Thioredoxin nuclear translocation and interaction with redox factor-1 activates the activator protein-1 transcription factor in response to ionizing radiation. *Cancer Res* 60: 6688–6695, 2000.

Address reprint requests to:
Dean P. Jones
615 Michael St., Suite 205P
Atlanta, GA 30322

E-mail: dpjones@emory.edu

Date of first submission to ARS Central, December 4, 2006; date of revised submission, February 19, 2007; date of acceptance, March 5, 2007.

This article has been cited by:

1. Marc Fransen, Marcus Nordgren, Bo Wang, Oksana Apanasets. 2012. Role of peroxisomes in ROS/RNS-metabolism: Implications for human disease. *Biochimica et Biophysica Acta (BBA) - Molecular Basis of Disease* **1822**:9, 1363-1373. [CrossRef]
2. Sarit Anavi, Noga Budick Harmelin, Zecharia Madar, Oren Tirosh. 2012. Oxidative stress impairs HIF1# activation: a novel mechanism for increased vulnerability of steatotic hepatocytes to hypoxic stress. *Free Radical Biology and Medicine* **52**:9, 1531-1542. [CrossRef]
3. Mamiko Ikeda, Hidehiko Nakagawa, Takayoshi Suzuki, Naoki Miyata. 2012. Novel bisbenzimide-nitroxides for nuclear redox imaging in living cells. *Bioorganic & Medicinal Chemistry Letters* . [CrossRef]
4. Bryan C. Dickinson, Yan Tang, Zengyi Chang, Christopher J. Chang. 2011. A Nuclear-Localized Fluorescent Hydrogen Peroxide Probe for Monitoring Sirtuin-Mediated Oxidative Stress Responses In Vivo. *Chemistry & Biology* **18**:8, 943-948. [CrossRef]
5. Jacqueline M. Heilman, Tom J. Burke, Craig J. McClain, Walter H. Watson. 2011. Transactivation of gene expression by NF-#B is dependent on thioredoxin reductase activity. *Free Radical Biology and Medicine* . [CrossRef]
6. Linda E Kippner, Nnenna A Finn, Shreya Shukla, Melissa L Kemp. 2011. Systemic remodeling of the redox regulatory network due to RNAi perturbations of glutaredoxin 1, thioredoxin 1, and glucose-6-phosphate dehydrogenase. *BMC Systems Biology* **5**:1, 164. [CrossRef]
7. Barry R. Imhoff, Jason M. Hansen. 2010. Tert-butylhydroquinone induces mitochondrial oxidative stress causing Nrf2 activation. *Cell Biology and Toxicology* **26**:6, 541-551. [CrossRef]
8. D. P. Jones, Y.-M. Go. 2010. Redox compartmentalization and cellular stress. *Diabetes, Obesity and Metabolism* **12**, 116-125. [CrossRef]
9. Young-Mi Go , Dean P. Jones . 2010. Redox Control Systems in the Nucleus: Mechanisms and Functions. *Antioxidants & Redox Signaling* **13**:4, 489-509. [Abstract] [Full Text HTML] [Full Text PDF] [Full Text PDF with Links]
10. Y GO, D JONES. 2008. Redox compartmentalization in eukaryotic cells. *Biochimica et Biophysica Acta (BBA) - General Subjects* **1780**:11, 1273-1290. [CrossRef]
11. Melissa Kemp, Young-Mi Go, Dean P. Jones. 2008. Nonequilibrium thermodynamics of thiol/disulfide redox systems: A perspective on redox systems biology. *Free Radical Biology and Medicine* **44**:6, 921-937. [CrossRef]